DRD No. SE-5
DRL No. 139

LARGE AREA SHEET TASK

ADVANCED DENDRITIC WEB GROWTH DEVELOPMENT

Quarterly Report

JPL NO. 9950-511

October 23, 1980 to December 31, 1980

DOE/JPL-955843/81/1
DIST. CATEGORY UC-63

C. S. Duncan, R. G. Seidensticker, J. P. McHugh
R. H. Hopkins, D. Meier, E. Frantti, and J. Schruben

Contract No. 955843

January 31, 1981

The JPL Low-Cost Silicon Solar Array Project is sponsored by the U. S. Dept. of Energy and forms part of the Solar Photovoltaic Conversion Program to initiate a major effort toward the development of low-cost solar arrays. This work was performed for the Jet Propulsion Laboratory, California Institute of Technology by agreement between NASA and DOE.

Westinghouse R&D Center
1310 Beulah Road
Pittsburgh, Pennsylvania 15235

TECHNICAL CONTENT STATEMENT

"This report was prepared as an account of work sponsored by the United States Government. Neither the United States nor the United States Department of Energy, nor any of their employes, nor any of their contractors, subcontractors, or their employees, makes any warranty, express or implied, or assumes any legal liability or responsibility for the accuracy, completeness or usefulness of any information, apparatus, product or process disclosed, or represents that its use would not infringe privately owned rights."

Dwg. 7734A51

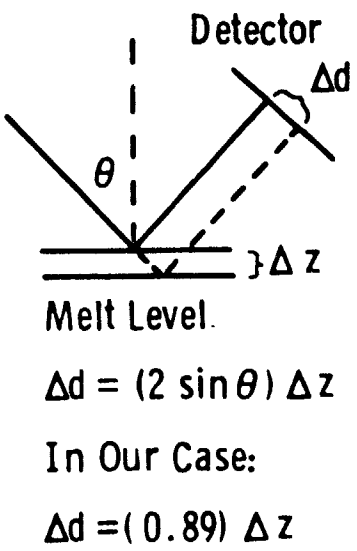

Figure 2 Magnified view of the way in which the laser beam position shown in Figure 1 changes with melt level.

2. INTRODUCTION

This is the first Quarterly Report on JPL Contract No. 955843 entitled "Advanced Dendritic Web Growth Development." The overall objective is to demonstrate the technology readiness of the silicon dendritic web process to produce sheet material at a cost compatible with the DOE/JPL goal of $0.70 per peak watt of photovoltaic output power in 1986.

Silicon dendritic web is a ribbon form of silicon grown directly from the melt without dies or shapers and which produces solar cells with AM1 conversion efficiencies above 15%. Most of the technical requirements to meet the 1986 cost goals have already been demonstrated individually including area throughput rate, solar cell efficiency, melt replenishment with closed loop control and preliminary design of furnace hardware.[1]

The thrust of this program is to combine these developments and to design, fabricate and operate a prototype automated web growth machine to demonstrate technology readiness. This will include identification of cost reductions in the mechanical and electrical hardware, system test, and web growth under automated control. A parallel study is underway to further increase web output rate to 35 cm^2/min benefiting in added product cost reduction. Periodic updating of economic analyses will be made to reflect new cost and technical information as it becomes available.

This report covers the two month period between the contract inception in late October and the quarter's end, December 31, 1980. The main activities, equipment design, sensor and control refinement, and throughput-related activities, are described on the sections that follow.

3. TECHNICAL PROGRESS

3.1 Performance Refinements to Sensing and Control Equipment

3.1.1 Melt Level Control System

Under a previous contract[2] a method was developed for detecting the silicon melt level while a web crystal is being grown. The method involves reflecting the beam of a 2 mW Helium-Neon laser from the melt surface and then detecting this reflected beam with a silicon photodiode. The experimental set-up is illustrated in Figure 1. If Δz is the amount by which the melt level changes, Figure 2, then the corresponding change in the position at which the beam strikes the detector is given by:

$$\Delta d = (2 \sin\theta)\ \Delta z \qquad (1)$$

where θ is the angle of the incident beam relative to the normal, as shown in Figure 2. In our geometry we have:

$$\Delta d = (0.89)\ \Delta z \qquad (2)$$

The currents produced by the photodiode provided feedback information to a silicon pellet feed mechanism. In this way an automatic melt replenishment system was successfully demonstrated in which the melt level was held constant to within 0.1 mm for an eight-hour period while a web crystal was grown.

Although this system performed quite well, it was partly constructed from available laboratory equipment, and so is open to refinements in several areas. With an eye toward making the melt replenishment system more suitable to a production environment, the

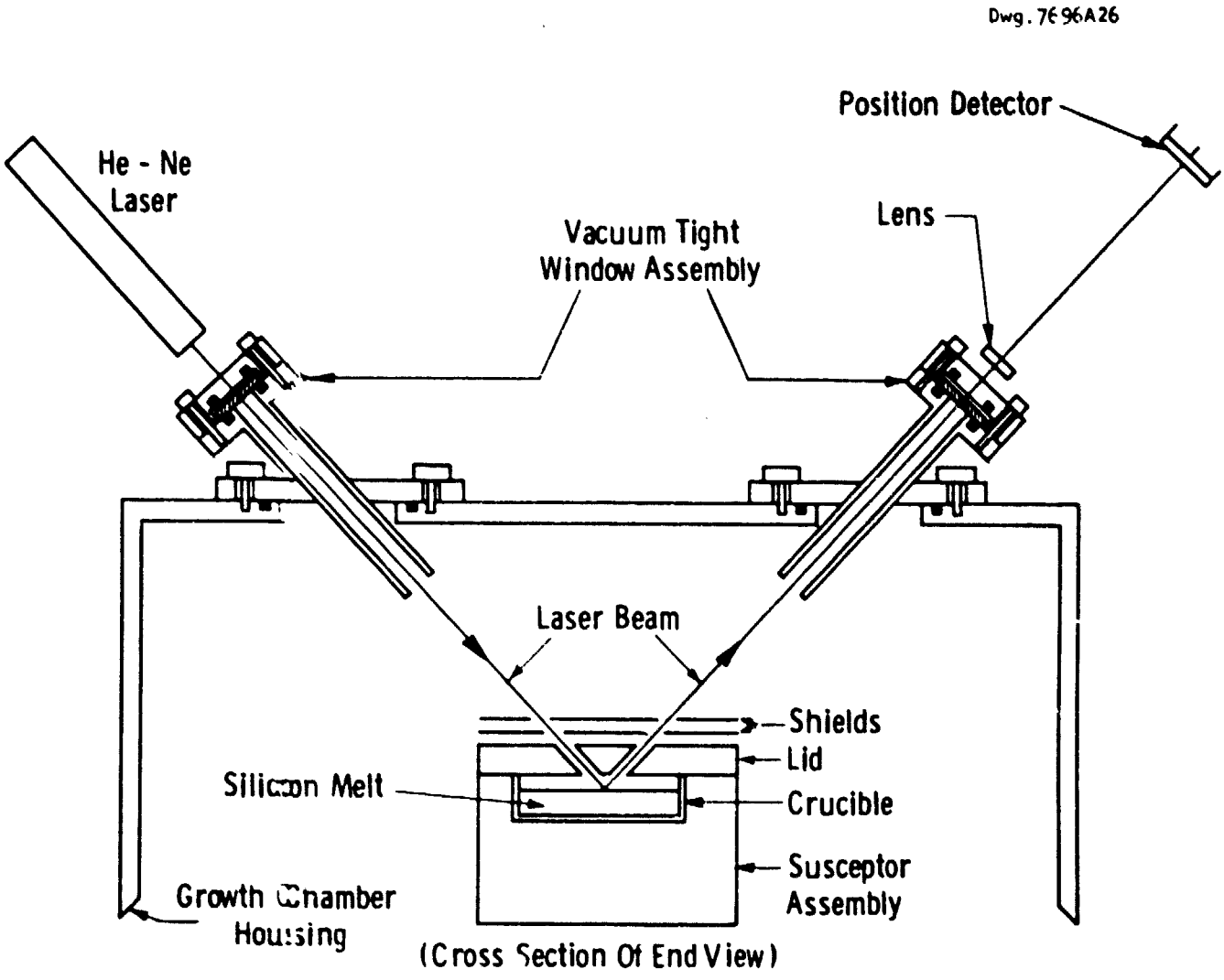

Schematic of melt level sensor

Figure 1 Schematic Depiction of Melt Level Sensor for Web Growth

Dwg. 7734A51

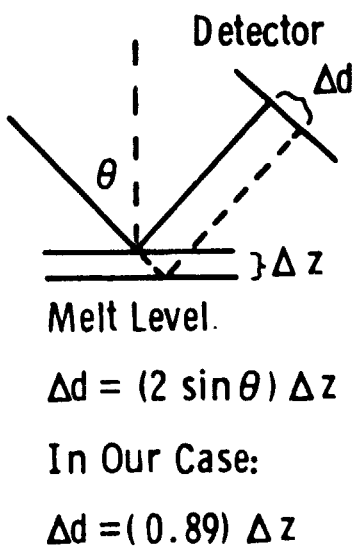

Figure 2 Magnified view of the way in which the laser beam position shown in Figure 1 changes with melt level.

following refinements were thought to be desirable:

1. The melt level sensing signal should be made relatively insensitive to variation in the intensity of the detected beam. Such variations will occur, to some degree, as the windows in the web growth furnace become clouded with oxide.

2. Fluctuations in the melt level sensing signal, which arise from the shimmering of the melt surface, should be smoothed to give a signal with less noise.

3. The speed of the gearmotor which drives th pellet feed mechanism should be continuously variable. This would ensure a smooth tracking of the pellet feed rate with the web growth rate and would disturb the steady state thermal growth conditions to a minimal extent. It would also permit an automatic shutdown of the pellet feed mechanism if web growth were to be unintentionally interrupted for any reason.

The design of a revised melt replenishment control system which incorporates these three refinements has been completed. It is shown in block diagram form in Figure 3. The silicon photodiode detector is represented as two back-to-back diodes with common anodes in Figure 3. This simply reflects the fact that the total current generated by the incident laser beam divides and flows along two separate paths to the two ends of the photodiode detector. If the laser beam strikes the center of the 3 cm long photodiode, the current (I_1) that flows along the diffused layer of the diode to one current-collecting end will be equal to the current (I_2) that flows in the opposite direction to the other current-collecting end. In this case the difference between these currents (I_1-I_2) is zero, indicating that the laser beam has struck the detector at its center.

In general, the magnitudes of the two currents will be determined by the relative distances that the charges must flow from the point of their creation to the two ends of the photodiode.

Dwg. 7734A48

BLOCK DIAGRAM OF MELT REPLENISHMENT CONTROL SYSTEM

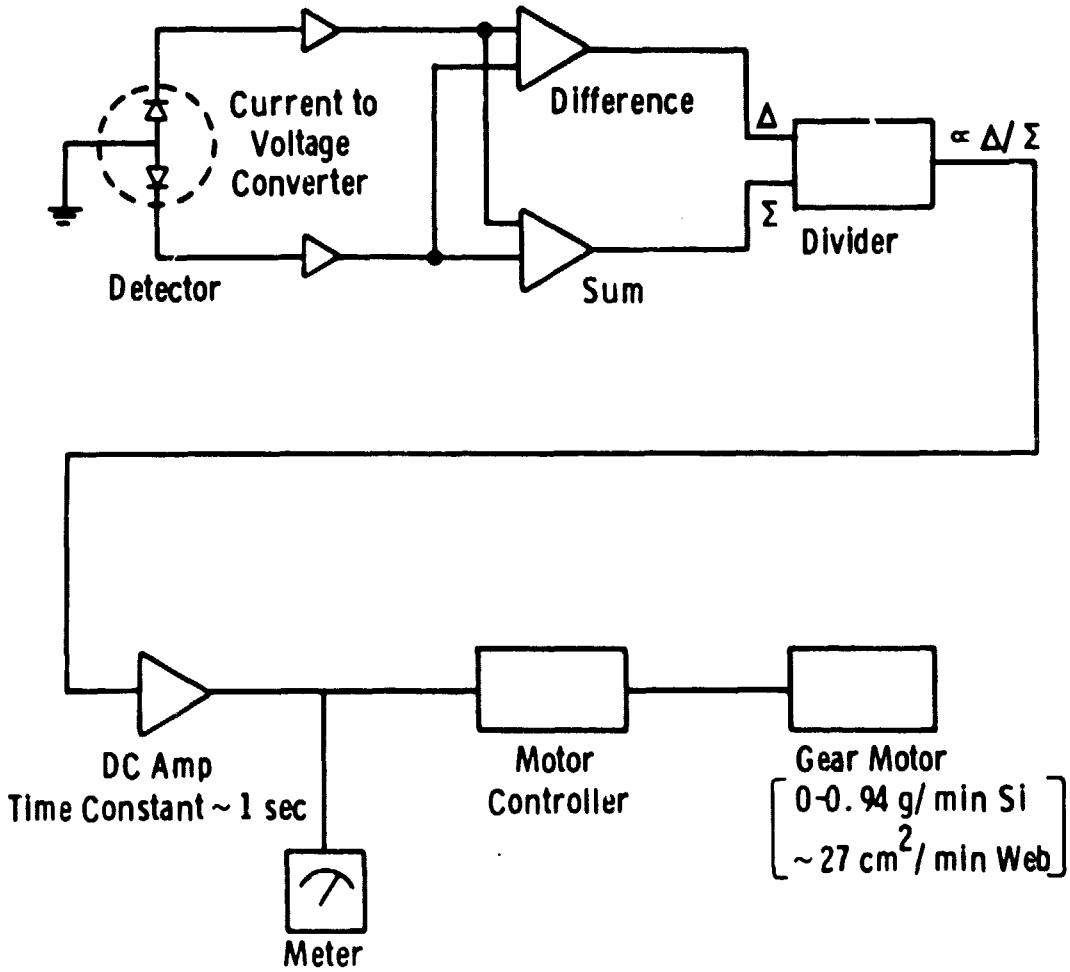

Figure 3 Block diagram of refined melt replenishment control system.

In addition, the power of the laser beam P(mW) and the response of the photodiode at the laser wavelength R(λ) (mA/mW) directly determine the magnitudes of the photocurrents produced. If L is the total length of the photodiode and ℓ_1 is the distance between the end from which I_1 flows and the point at which the laser beam is incident, then the difference in the two currents is given by:

$$\Delta I = (I_1 - I_2) = PR(\lambda)\ (1-2\ell_1/L) \qquad (3)$$

Thus the difference current (ΔI) provides a signal which is linearly related to the positions of the incident laser beam (ℓ_1).

It is this difference current that was used as the feedback signal to control the speed of the silicon pellet feed mechanism in the original version of the melt replenishment system.[2] However, as can be seen from Equation 3, this difference current depends on the intensity of the laser beam (P) as well as upon the position of the beam (ℓ_1). This dependence on intensity can be removed if a second signal, equal to the sum of the two currents is simultaneously generated. This sum signal (ΣI) depends only on laser power P and detector response R(λ) and is independent of the position of the beam. It is given by:

$$\Sigma I = (I_1 + I_2) = PR(\lambda) \qquad (4)$$

As can be seen from Equations 3 and 4, if the difference current is normalized by the sum current to form a signal, then this signal is independent of laser beam intensity and detector response. Dividing Equation 3 by Equation 4 we obtain the normalized difference current:

$$\Delta I/\Sigma I = (1-2\ell_1/L) \qquad (5)$$

As shown in Figure 3, this approach is implemented by converting the diode currents to voltages and forming the sum and difference signals with the aid of operational amplifiers. The normalized difference signal (Δ/Σ) is then obtained by using an analog divider integrated circuit.

It should be pointed out that in arriving at Equations 3 and 4 it was assumed that the photogenerated charge travels along the diffused layer of the photodiode without recombination. This is an oversimplification since in the steady state some carriers are reinjected across the photodiode junction into the base region where they are lost by recombination.[3] When this effect is taken into account[4] one arrives at an expression for ΔI which is more complicated than Equation 3 but which does reduce to Equation 3 in certain limits.

The amplified sum and difference signals were measured as a function of beam position in the photodiode as part of a laser/detector bench test. The results are shown in Figure 4. There it is seen that over the central portion of the detector the condition of a linearly-varying difference signal (Equation 3) and a constant sum signal (Equation 4) is valid. From the data of Figure 3, the quotient (Δ/Σx10) was computed to simulate the action of the analog divider of Figure 3. These results are given in Figure 5 where it is shown that the analog divider serves to extend the linear range of the photodiode to nearly its full length in addition to providing a signal which is relatively insensitive to beam intensity.

The second refinement to the original melt replenishment system involves smoothing the fluctuations in the melt level signal which arise from the shimmering of the melt surface. This is done with the aid of a DC amplifier whose time constant is 1 second as shown in Figure 3. This is a period of time which is sufficiently long to average the noise to zero yet sufficiently short to permit response to time changes in the melt level.

The final refinement is to provide for a continuously variable pellet feed rate. As shown in Figure 3, this is achieved simply by supplying the output signal from the DC amplifier to a controller for the gearmotor which rotates the pellet feed mechanism. The gearmotor of choice has a maximum speed corresponding to a silicon mass input rate of 0.94 g/min and a web growth rate of approximately 27 cm^2/min. If this feedrate proves to be inadequate at some future time, the simple replacement of only the gearmotor will provide an expanded range.

Curve 725245-A

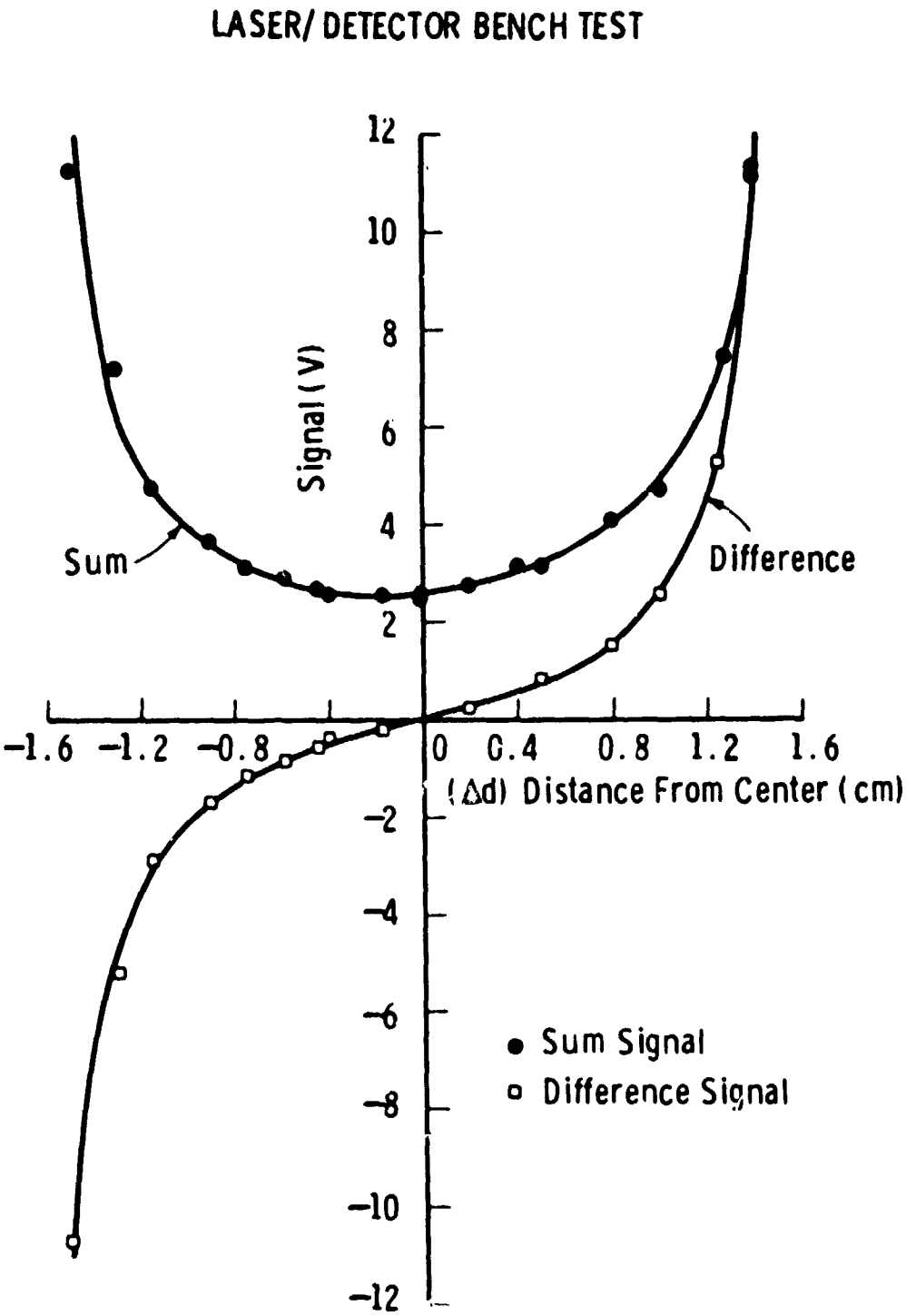

Figure 4 Sum and difference signals of position detector

Curve 725244-A

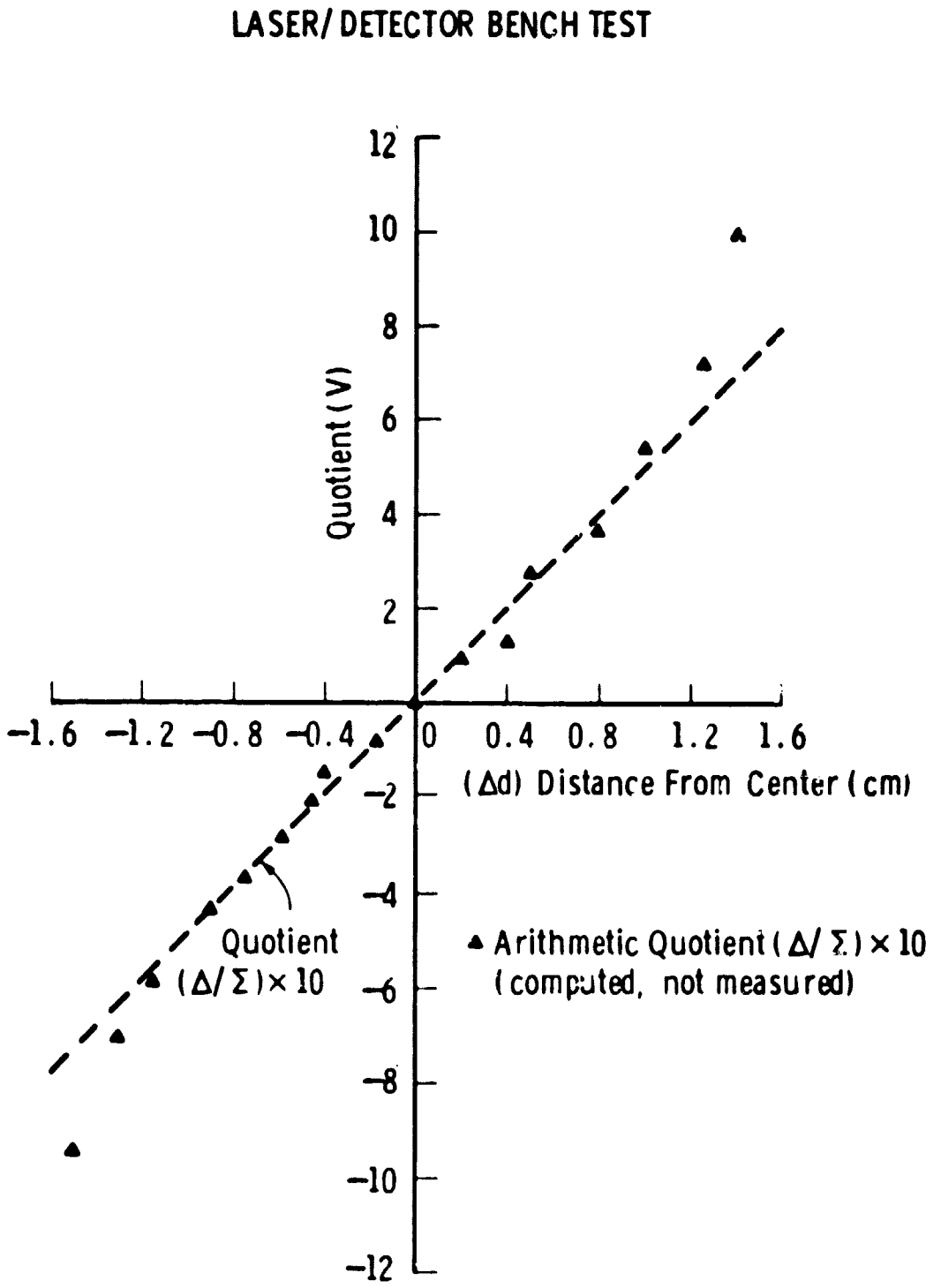

Figure 5 Normalized difference signal

With the exception of the gear motor and its controller the system as shown in Figure 3 was assembled and bench-tested. In the bench test the detector responded to a direct laser beam rather than a reflected beam. The system performed satisfactorily, with the noise at the output of the DC amplifier being equivalent to an uncertainty in the melt level position of less than 0.01mm. The gear motor and its controller have been ordered and are scheduled to be shipped shortly. With the receipt of these two componenets the system can be fully assembled and then tested during a web growth run.

3.1.2 Dendrite Thickness Sensor

The dendrite thickness of a growing web crystal is a sensitive indicator of the thermal conditions in the silicon melt. It can thus serve as a direct indication of growth conditions. Ultimately, the output from a circuit which detects the dendrite thickness could be used to control the temperature of the melt. In this way, compensation could be made for effects which are difficult to monitor directly, such as the changing emissivity of the lid and shields. The sensor would be of more immediate use as a process diagnostic for equipment development.

Several possible methods for detecting dendrite thickness have been considered. At this time the most promising method is one in which the growing web is viewed edge-on by a linear array of photodiodes. Using the glowing melt as a light source, a lens system can be used to magnify the image of the dendrite and focus it on the diode array outside the growth furnace.

Diode arrays and their associated control circuitry are commercially available at reasonable cost with a sensitivity and resolution that are quite adequate for our purposes. Thus far, a preliminary design of the lens system has been made and the required photodiode array and associated composites have been identified. This approach for measuring dendrite thickness will be further investigated.

3.1.3 Programmed Growth Initiation

It has been recognized that a controlled and reproducible start-up sequence is desirable for reliable, routine web growth. The start of growth has always been manually performed and is perhaps the most skill-demanding of the remaining manually performed operations. In routine web growth, there is experimental evidence that the start of growth can be automatically programmed. There is, therefore, the potential that growth can be initiated more consistently, a benefit in terms of improved web quality and reduced labor content in the operation.

Typically the growth initiation involves several minutes of coupled changes in melt temperature and growth velocity as suggested schematically in Figure 6. The melt is first undercooled below the equilibration or "hold" temperature T_H to produce a button of suitable width.[1,2] The growth velocity is increased to thin the button and start web propagation. Both temperature and velocity are then adjusted to their final steady-state values.

Clearly these manual operations can be carried out automatically by suitable equipment. We have loaded a typical temperature-velocity sequence like that depicted in Figure 6 into an L and N process programmer. To facilitate transfer of signals to the growth equipment an interface between the process programmer and the pull speed has been designed and constructed. The interface has been tested and the programmer was able to step the speed control through the complete sequence shown in the figure. The interface between programmer and the temperature control has not yet been completed. That should be accomplished shortly and a programmed initiation of crystal growth experiment is anticipated in the near future.

3.2 Design of Prototype Web Growth Machine

This work is a continuation of design started under JPL Contract 954654.[1] The task is comprised mainly of mechanical and electronic design which, to a considerable degree, can be performed independently. In each of these design areas the initial work emphasis is placed on satisfying

Curve 725246-A

TYPICAL PROGRAM SEQUENCE FOR WEB GROWTH INITIATION

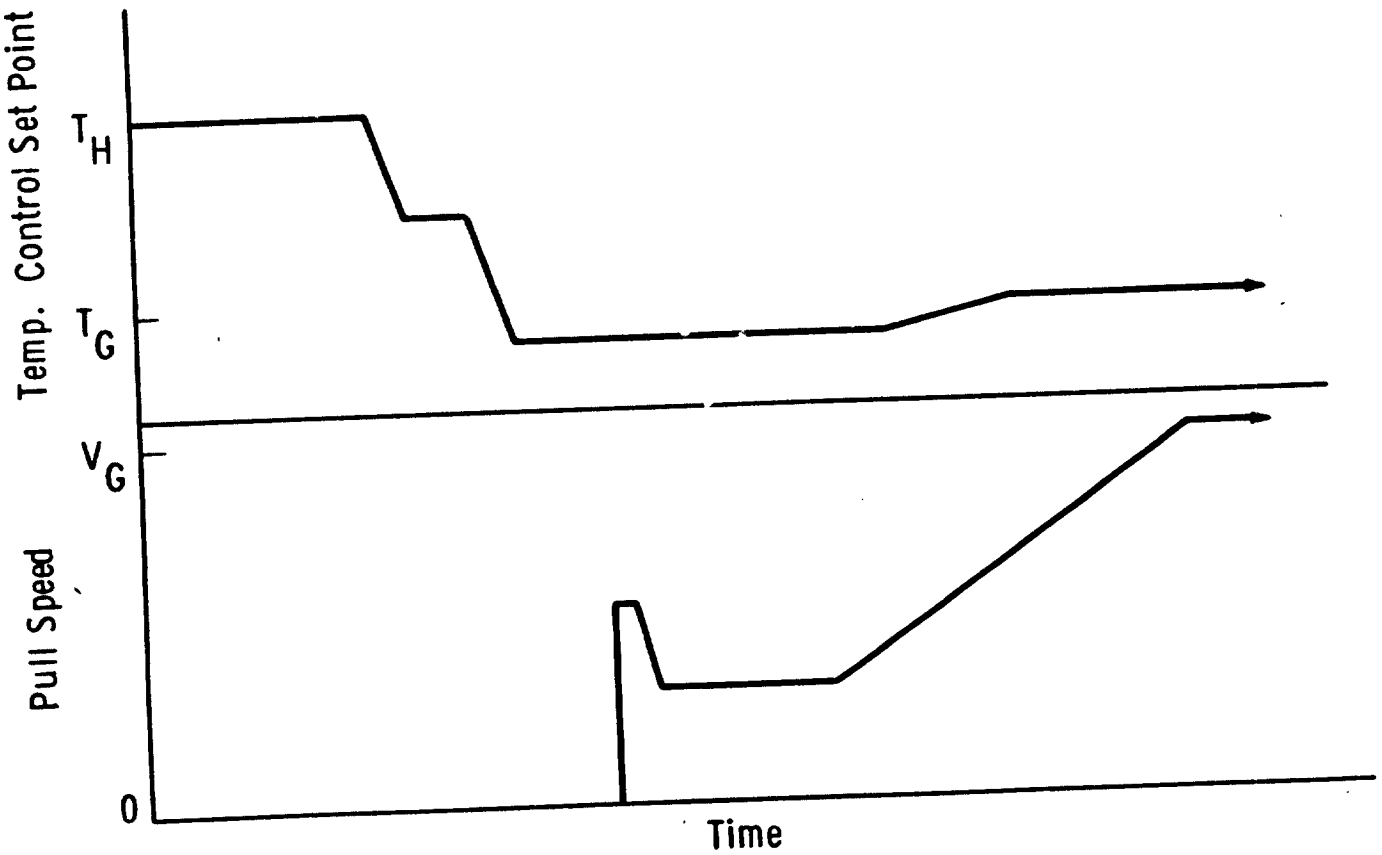

Figure 6 Typical program sequence for web growth initiation

the functional requirements of the apparatus. Subsequently the design is refined with respect to the cost of the apparatus while maintaining its fit and function within the overall design. A preliminary design review was held November 18, 1980 at JPL.

3.2.1 Mechanical Design

The mechanical design to satisfy all the apparatus functional requirements has been completed and design refinements for the purpose of reduction of equipment cost have been started. Current effort is directed at design refinment of the growth chamber and the growth/storage reel, where large cost reductions are expected.

3.2.2 Electronic Design

Besides the improvements in the functional design of certain electronic equipment (Section 3.1) we are also reviewing certain aspects of the control equipment for cost reduction. For example, the temperature control equipment used in this program fully satisfies the functional requirements of the process but, because it was originally specified for its versatility, has costly features not required for web growth. Consequently, this equipment is unnecessarily expensive, and an effort has been started to specify or, if necessary, design low cost control circuitry having only those features required for web growth.

The specifications for a temperature controller, derived from the present system, are as follows: an input range of -1 mV to +1 mV for an output range of 0 to 5 milliamperes, a zero adjustment from 40 to 50 mV on the input signal, and a reset action of 0.5 to 1 repeat per minute.

A number of controller manufacturers have been contacted to survey available equipment and as a result of these discussions, it appears at this time that the temperature control requirements can be met at a cost less than that specified in the economic analysis for a low cost web growth facility.

Arrangements have been made to secure a simple controller from one manufacturer, L&N, on a loan basis. This controller appears to meet the required specifications and we anticipate testing its functional capabilities during the next reporting period.

3.3 Advanced Throughput Development

3.3.1 Introduction

The objective of this activity is to provide increased web throughput rates-up to 35 cm^2/min-and thus reduce sheet cost further. The experimental effort includes: (1) the demonstration of higher throughput in terms of cm^2/min and (2) the development of the necessary technology for long growth runs at high throughput rates.

The first activity involves continued evolution and testing of lid and shield designs for higher growth velocity and for the reductions of the stress which tends to limit width via elastic deformation. The second involves equipment design, degree of automation, long-term stability, melt level maintenance, and all those factors which are pertinent to sustaining the desired thermal condition in the growing web for long time periods, including the control of the width of a growing web crystal.

3.3.2 Enhanced Area Throughput

During this reporting period, laboratory activities have been directed towards increased growth velocity and control of crystal width. As results from the thermal modeling efforts related to elastic stress become available, (see Section 3.3.3) they will be integrated into the experimental effort so that the technology developed in the growth velocity and width control activities will be applied to the growth of web crystals of increasing width.

In order to increase growth velocity, a series of experiments with thinner lids has been initiated. A thin lid has the effect of increasing radiative losses from the web near the growth interface so that the heat of fusion is more rapidly dissipated, thus permitting

more rapid growth for a given crystal thickness. Previous work has shown that simply thinning the lid, while having a large effect on growth velocity, can have negative effects in terms of crystal quality and oxide deposition. These effects occur because a thin lid tends to run colder in the region of the growth slot. Thus, concurrent changes must also be made in the top shield configuration in order to provide a vertical temperature distribution which not only produces substantially higher growth velocities, but also maintains good growth behavior in terms of growth initiation, crystal quality and freedom from oxide interference. To accomplish this series of experiments are being undertaken in which the lid is systematically thinned in steps while changes are made in the top shield configuration to maintain good quality growth.

Initial experiments involved an RE-1[1] lid reduced in thickness by 20%, with the RE-1 shield arrangement. As expected, growth velocity increased significantly as determined by thickness-velocity measurements.[1] In terms of the relationship

$$V = c + \frac{d}{t}$$

which relates growth velocity (V) to web thickness (t) both coefficients c and d increase when compared to the original thicker lid designs. However, growth initiation was difficult and stability and crystal quality poor. The addition of two more top shields to this configuration resulted in stable growth with some tradeoff in maximum growth velocity.

Some other variations in the number and spacing of top shielding using the same lid have been tested. Only small effects were found in terms of growth velocity, but these experiments have led to the development of several important guidelines relating to lid and shield configuration which if not considered may produce unwanted side effects, for example sporadic floating ice and growth inhibiting oxide accumulation in the slot region of the shields. The configurational parameters to be controlled are the lid temperature and the spacing between the various components of the lid-shield stacks. By maintaining the bottom of the lid at sufficiently high temperature and keeping appropriate top shield spacing, oxide and ice are prevented.

The lid temperature can be controlled to the required degree by adequate radiation shielding and by proper positioning of the work coil. In addition, the lid bottom and susceptor top must mate well to insure maximum contact and thus maximum heat transfer between the two. When conditions are properly controlled in terms of shielding, lid-susceptor fits, etc, the lid bottom is totally free of oxide deposits and ice from spalling does not occur.

One of the important aspects of top shield spacing is the separation between the lowest shield and the lid. If this spacing is too small, oxide is deposited on the shields and grows out over the slot region, inhibiting crystal growth. The minimum spacing needed to prevent such oxide deposition appears to be about 4.5mm. This observation had previously been made relative to the J-181 lid and shield configuration, in which the lowest top shield is thin and relatively cold. Recent experiments indicate that this spacing requirement is much more general and that the temperature per se is not the only factor to consider; the convective gas flow patterns are critical in relation to growth inhibiting oxide deposition on the top shields.

Another observation relative to shield spacing relates to the spacing between the individual shields in multiple shield stacks. A spacing of 1.5mm is generally satisfactory. Expanding this spacing to 3mm can cause the deposition of a hard blue oxide on the web crystal (as opposed to the normal fluffy easily-removed type). Again, in this case, the convective gas flow patterns are believed to be significant. In order to allow flexibility in the design of shield configuration we plan to test the effect of baffles between the shields for the purpose of modifying convective flow patterns.

Experiments related to web width control were carried out using modifications of the J-181 and RE-1 lid and shield configurations. Width control is critical to the goal of enhanced long duration throughput and to the operation of the automated growth facility later in this contract. Width control has previously been demonstrated,[1,2] but those demonstrations

involved the continuous attention of a skilled operator. The goal of the present effort is to develop configurations which will allow a web crystal to reach a predetermined width, then hold at that width without active participation of the operator, i.e.—passive width control.

Our experiments thus far show that passive design configurations can indeed limit crystal width, but we have not yet been able to maintain passive control for extended periods of time. We have, however, been able to maintain greatly reduced widening rates, so that much longer sections of crystal fall within a selected range of width.

3.3.3 Thermal Stress Modeling and Analysis

Thermally generated stresses have two major effects on the growth of ribbon crystals including dendritic web: residual stresses in the grown crystal and deformation or "buckling" during growth.[5] There is good evidence that the lateral stress, σ_{yy}, near the growth front is the primary source of the residual stress, while the longitudinal stresses, σ_{xx}, away from the growth front is responsible for the buckling deformation. In practice, the residual stresses can be controlled by tailoring the thermal environment near the growth front by proper design of lid slot configuration and control of the melt height.[2]

Even when residual stresses are not a problem, buckling still occurs when the web has reached some critical combination of width and thickness. So far control of the stresses causing buckling has not been obvious. Our goal in the present program is to identify the critical buckling stress magnitude, the temperature profile necessary to avoid deformation, and finally the growth configuration required to generate this profile.

Unlike the residual stress, resulting from plastic deformation of the ribbon, the stresses causing buckling are affected by the temperature distribution away from the interface region. R. W. Gurtler[6] has modeled the stresses from two temperature distributions which were identical near the melt surface, but different at greater distances.

The first distribution decreased linearly along the length of the ribbon; there was no elastic stress and there would be no buckling. Unfortunately, this temperature distribution is unrealistic since absolute zero is reached a few centimeters from the growth front. The temperature decline could not be made more gradual without excessively slowing the growth rate.

The second temperature distribution was identical to the first near the growth front but parabolically approached ambient temperature instead of linearly reaching absolute zero; this temperature profile caused large elastic stresses.

Of course, the mere existance of thermal stresses in a glowing web crystal does not automatically mean that the web will have residual stresses or deform during growth. In order for residual stress to be observed, the thermal stress must have exceeded the yield stress; for deformation to occur, the thermal stresses must exceed some critical buckling stress. A determination of the buckling stress criterion and the required temperature distribution would be a valuable guide in the design of high throughput growth configurations. The following sections review the mathematical formulation of both thermal stress generation and the ribbon deformation and elucidate several approaches to solving the problems.

Stress model. The stresses in a thin ribbon of thickness t, length coordinate x, and width coordinate y, are related to the plane temperature distribution T (x,y) by means of the Airy stress function ϕ:

$$\sigma_{xx} = \frac{\partial^2 \phi}{\partial y^2}$$

$$\sigma_{xy} = - \partial^2 \phi / \partial_x \partial y \qquad (6)$$

$$\sigma_{yy} = \partial^2 \phi / \partial_x{}^2$$

where σ_{xx} is the longitudinal stress, σ_{xy} is the shear stress and σ_{yy} the transverse stress. These stresses are determined from the temperature distribution via the differential equation

$$\Delta^2\phi = -\alpha E \Delta T \tag{7}$$

where α is the thermal expansion coefficient, E is the modulus of elasticity (Young's modulus),

$$\Delta \equiv \frac{\partial^2}{\partial x^2} + \frac{\partial^2}{\partial y^2} + \frac{\partial^2}{\partial z^2}$$

is the Laplacian or harmonic operator and Δ^2 is its square or the biharmonic operator. Boundary conditions require that both ϕ and its normal derivative should vanish on the growth front and on the edges of the web.

With proper shield design the web temperature should be nearly constant in the crosswise, or y, direction. For this case, $T = T(x)$, Boley and Wiener[7] have found an approximate series solution for Equation 2 which is valid away from the melt surface. Numerical solutions can also be obtained by various techniques; for example, the Westinghouse WECAN finite element code has been used to solve for the stress distribution both near and far from the growth front with an arbitrary temperature distribution for input.[1]

Buckling Model. Whether or not the stresses determined by Equation 2 would cause buckling depends on another differential equation which also involves the biharmonic operator:[8]

$$\frac{t^3 D \Delta^2 w}{12(1-\nu^2)} = \sigma_{xx}\frac{\partial^2 w}{\partial x^2} + \sigma_{yy}\frac{\partial^2 w}{\partial y^2} + 2\sigma_{xy}\frac{\partial^2 w}{\partial x \partial y} \tag{8}$$

where ν is Poisson's ratio, E is Young's modulus, and $w(x,y)$ is the transverse deflection (z direction) of a buckled thin plate of thickness t. The system of equations (6), (7), and (8) under the appropriate boundary conditions form the mathematical model of buckling in silicon web growth.

Since the web edges consist of dendrites which are less flexible than the web itself, the closest model for the boundary conditions would seem to be edges supported by elastic beams:[8]

$$EI \frac{\partial^4 w}{\partial x^4} = \pm D \left| \frac{\partial^3 w}{\partial y^3} + (2-\nu) \frac{\partial^3 w}{\partial x^2 \partial y} \right| + A \sigma_{xx} \frac{\partial^2 w}{\partial x^2} \qquad (9)$$

$$+ A \frac{\partial \sigma_{xx}}{\partial x} \frac{\partial w}{\partial x}$$

on the edges $y = \pm c$, where EI is the flexural rigidity of the dendrite, A is the cross-sectional area of the dendrite and $D = ET^3/ 12(1-\nu^2)$ is the flexural rigidity of the plate or web. Here we have added the last term on the right side of Equation (9) to account for the longitudinal variation of σ_{xx}. Equation (9) accounts for the twisting moments and the vertical shearing forces at the edges. The bending moments are considered in an additional bondary condition:

$$I C \frac{\partial}{\partial x} \left(\frac{\partial^2 w}{\partial x \partial y}\right) = D \left(\frac{\partial^2 w}{\partial x^2} + \nu \frac{\partial^2 w}{\partial y^2}\right. \qquad (10)$$

on $y = \pm c$, where C is the torsional rigidity of the dendrite.

For the edge of the initial button, boundary conditions similar to (9) and (10) would be appropriate when the growth has recently begun. After the web is long enough to wrap around the pickup reel, the leading edge of the web would be fixed and the boundary conditions would then be

$$w = \partial w/\partial x = 0 \qquad (11)$$

Finally, at the growth front $x = 0$, the edge is free and the boundary conditions are:

$$\left.\begin{aligned} \partial^3 w/\partial x^3 + (2-\nu)\ \partial^3 w/\partial x \partial y^2 &= 0 \\ \partial^2 w/\partial x^2 + \nu \partial^2 w/\partial y^2 &= 0 \end{aligned}\right\} \qquad (12)$$

Solution Methods

The WECAN program can solve Equations (6) - (12) for any arbitrary temperature distribution. (The problem of designing a furnace configuration to produce a desired temperature distribution will be considered after it is learned what the desired distribution is). Unfortunately, finding a solution for Equations (6)-(8) does not solve the buckling problem. In fact, the trivial solution, $w \equiv 0$, is such a solution; it represents the non-buckled state. As long as no other solution exists, there can be no buckling. The problem thus is to determine the range of temperature distributions which induce sufficiently low stresses such that Equations (6)-(12) have a unique solution, $w \equiv 0$. This range of temperature profiles will give leeway for proper silicon growth. We shall discuss four possible ways to approach this problem:

1) The WECAN computer program has the capability to solve eigenvalue problems and we can approximate the buckling problem as an eigenvalue problem by varying the stresses in a fixed proportion; i.e., let

$$\sigma_{xx} = \lambda \sigma^{\circ}_{xx}$$

$$\sigma_{yy} = \lambda \sigma^{\circ}_{yy}$$

$$\sigma_{xy} = \lambda \sigma^{\circ}_{xy}$$

where σ°_{xx}, σ°_{yy}, σ°_{xy} are the stresses determined from Equation (6) and (7) for some typical temperature distribution $T^{\circ}(x)$. WECAN can then determine the values of λ for which Equations (8)-(12) have a unique trivial solution. For these values of λ, any of temperature distributions, $\lambda T^{\circ}(x) + ax + b$ (a and b are independent of x and chosen to satisfy appropriate boundary conditions), would provide buckle-free silicon web growth. Notice that the second derivative of any of these distributions proportional to that of the initial temperature distribution.

Repetition of the above method for one or more initial temperature distribution (which are not proportional) could give some indication of the range of temperature distributions for which web growth would be stable.

2) Timoshenko and Gere[8] show how the eigenvalue problem mentioned in (1) can be solved as a minimization problem when series solutions to Equations (8)-(12) can be determined. They give series expansions for similar boundary problems. It is possible that these might be adapted to the problem at hand.

3) Similar to the energy method implied in (2) is functional analysis theory[9] for the uniqueness of solutions to the buckling differential equation. This theory may provide additional insight for determining the range of desirable temperature distributions for web growth.

4) Integral equations provide powerful methods for obtaining solutions to Equation (8)[10], however the complicated boundary conditions, Equations (9)-(12), make the analysis too difficult to pursue for the present.

Conclusions. We have presented several analytical approaches for establishing buckling criteria; they offer great power and generality but may take some time to develop. The numerical, finite element technique, can be used for solving a somewhat more restricted problem, but could yield results more quickly. We believe that under the time scale of the program, the finite element approach is the one that will be used, however a small level of effort will be continued on the most promising of the analytic methods.

3.4 Evaluation of Web Furnace Ambient

During the week of November 10-14, 1980 Prof. Darrell Ownby and Harold Romero visited our lab, per request by JPL, for the purpose of measuring the oxygen content of our ambient argon atmosphere. During

the previous week, we constructed a manifold with associated piping so that both the incoming gas and the ambient gas during growth runs in the RE and WA furnaces could be measured. Measurements were also made with different flow rates of the incoming gas to ascertain that low flow rates did not allow back diffusion of air through the furnace chimney. Preliminary results indicate that the oxygen partial pressures in both the incoming argon and in the furnace ambient during web growth are very low, $\sim 10^{-12}$ atm.

4. CONCLUSIONS

A detailed analysis of the melt level sensor and feed rate controller has been carried out and a circuit designed and built to (1) make the detection signal insensitive to the intensity of the laser beam reflected from the melt surface and (2) eliminate noise in the signal caused by vibration on the silicon melt surface. To assure smooth tracking of the pellet feed rate with the silicon consumed during web growth a continuously variable speed motor has replaced the older two-speed equipment.

Interfaces to present temperature and speed control equipment have been designed to permit programming of the initiation stage of web growth. The speed program has been successfully tested. When complete it is believed this approach will permit automation of the start-of-growth operation resulting in improved process reproducibility and reduced labor content.

Cost reduction studies are underway for the web furnace chamber and reel to identify functionally suitable but lower cost hardware. A temperature controller about one third as expensive as the current laboratory apparatus has been identified. It will be tested next month for fit and function.

Thinner lids and improved shield configurations have been designed to further increase throughput. Initial tests showed speed improvements as expected. In parallel with the experimental throughput related activities a limited amount of stress modeling is being carried out to identify criteria for web buckling which will lead to better lid designs. Emphasis here is on numerical approaches which should lead to a more rapid, but less detailed result than the analytical techniques.

5. PLANS FOR FUTURE WORK

During the coming quarter activity will continue in the areas of

1. furnace cost reduction,
2. design and assembly of hardware for the prototype automated furnace,
3. functional tests of electronic circuitry for temperature control and melt level sensing, and
4. improved throughput rate for web growth.

6. NEW TECHNOLOGY

No new technology is reportable for the period covered.

7. REFERENCES

1. C. S. Duncan, et al. Silicon Web Process Development, Final Report, DOE/JPL-954654-80/13.

2. C. S. Duncan, et al."Silicon Web Process Development Annual Report," June 30, 1980, Contract No. 954654, DOE/JPL-954654/80/11.

3. Gerald Lucovsky, J. Appl. Phys. 316, 1088 (1960).

4. William P. Conners, IEEE Trans. Electr. Dev. ED-18, 18, 59, (1971).

5. R. G. Seidensticker and R.H. Hopkins, "Silicon Ribbon Growth by Dendritic Web Process," J. of Crystal Growth 50 221-235, (1980).

6. R. W. Gurtler, "Nature of Thermal Stresses and Potential for Reduced Thermal Buckling of Thin Silicon Ribbon Growth at High Speed," J. of Crystal Growth 50, 69-82, (1980).

7. B. A. Boley and J. H. Weiner, Theory of Thermal Stresses (Wiley, New York, 1960) p. 261,320-324.

8. S. P. Timoshenko and J. M. Gere, Theory of Flastic Stability (McGraw-Hill, NY, 1961), p. 348-351, 332, 367.

9. G. Fichera, "Existence Theorems in Elasticity," Handbuch der Physik VIa/2 (1972) 347-389.

10. I. N. Vekua, New Methods for Solving Elliptic Equations (North-Holland-Amsterdam, John Wiley-New York, 1967) p 247-254.

8. ACKNOWLEDGEMENTS

We would like to thank, H. C. Foust, E. P. A. Metz, L. G. Stampahar, S. Edlis, W. B. Stickel, J.M. Polito, A. M. Stewart, J. P. Fello, and C. H. Lynn for their contributions to the web growth studies.

9. PROGRAM SCHEDULE AND COSTS

9.1 Updated Program Plan

9.1.1 Milestone Chart (attached)

9.1.2 Program Cost Summary (attached Curve 725242A)

9.1.3 Program Labor Summary (attached Curve 725243A)

9.2 Man-Hours and Costs

	Man-Hours		Costs
Previous	0	Previous	$ 0
This Period	3,613	This Period	$148,432
Cumulative	3,613	Cumulative	$148,432

DWG. 5594C76

LSA PROJECT
LARGE AREA SILICON SHEET
ADVANCED DENDRITIC WEB GROWTH DEVELOPMENT
MILESTONE CHART – JPL CONTRACT 955843

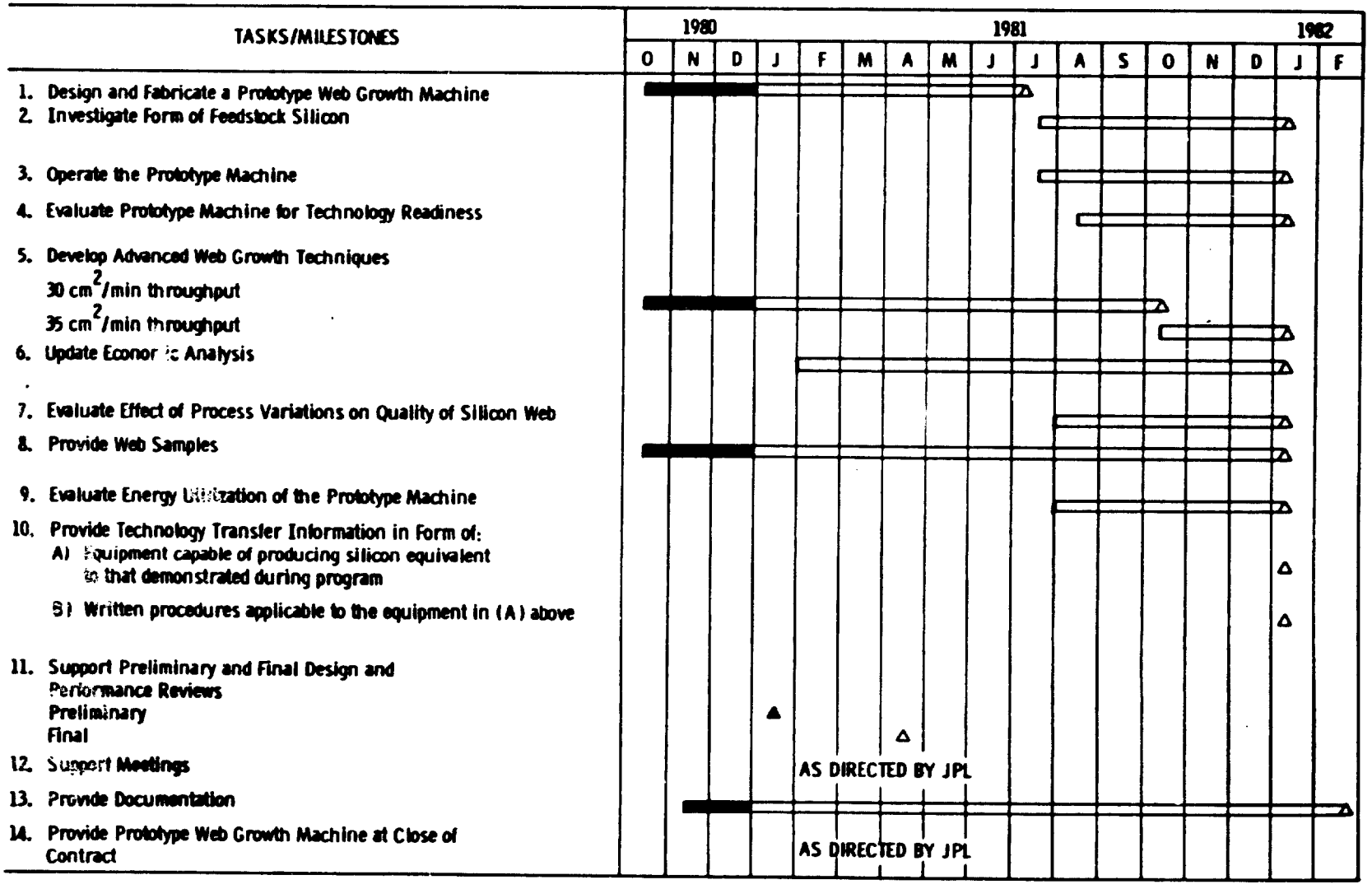

9.1.1 Milestone Chart

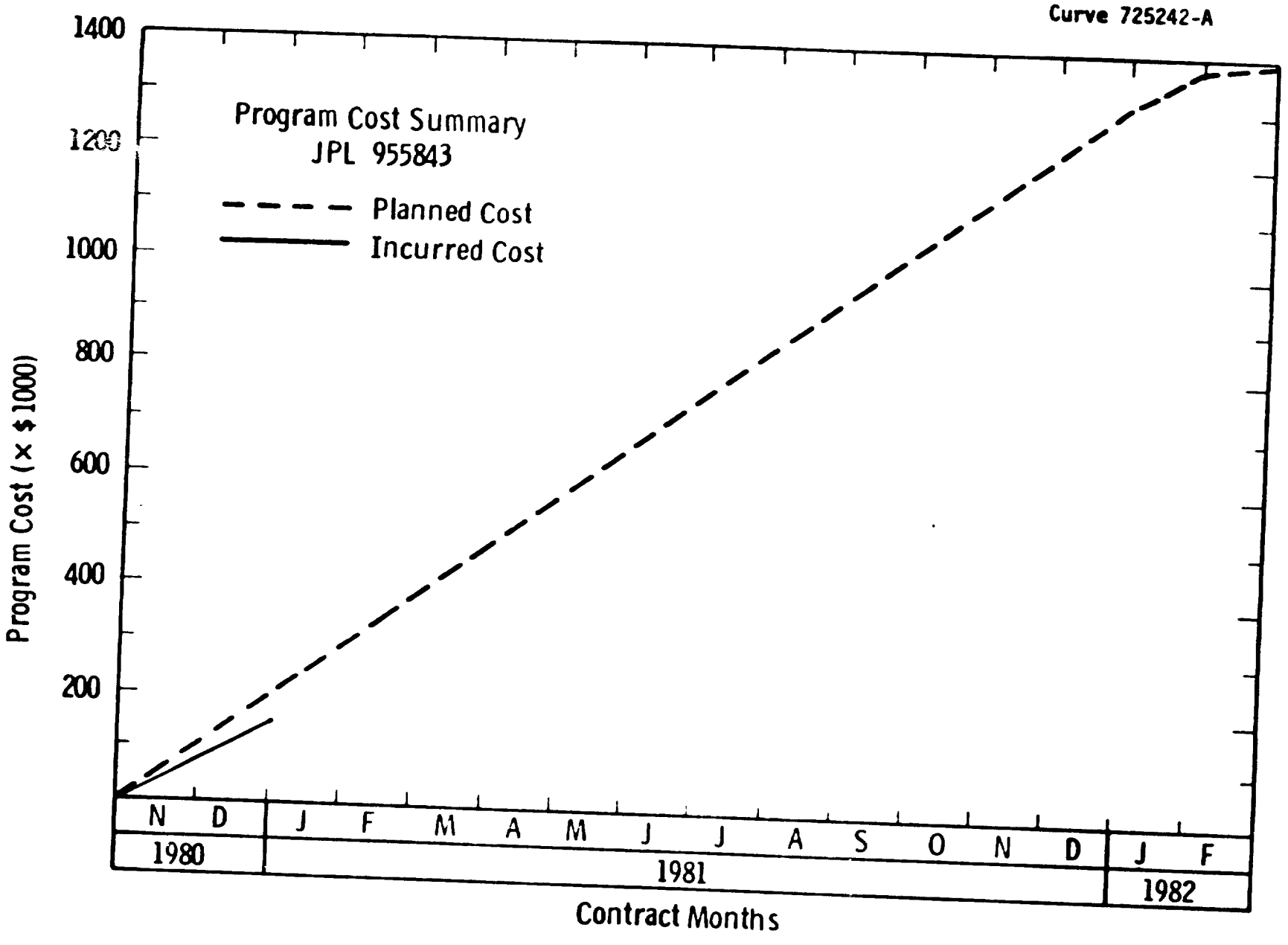

9.1.2 Cost Summary

Curve 725243-A

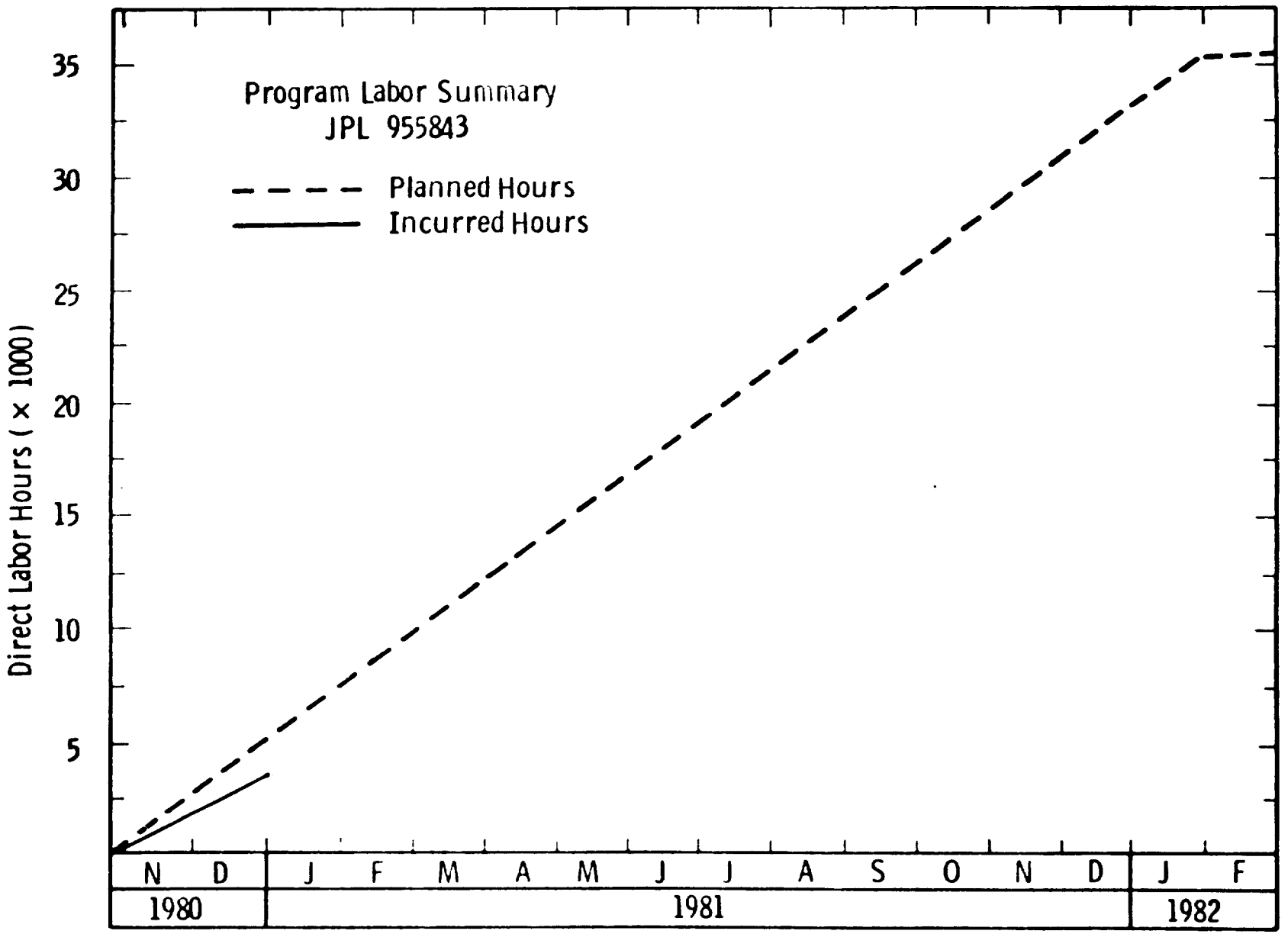

9.1.3 Labor Summary